Pflügers Arch (1986) 407:465–475

Pflügers Archiv
European Journal of Physiology

Sodium conductance in calcium channels of guinea-pig ventricular cells induced by removal of external calcium ions

Hiroko Matsuda*

National Institute for Physiological Sciences, Myodaiji, Okazaki 444, Japan

Abstract. An inward current characterized by a slow inactivation, was induced when the extracellular Ca^{2+} concentration was reduced by EGTA. It was suppressed by replacing external Na^+ with $Tris^+$ or by D-600, increased by epinephrine, and was not affected by TTX. These findings suggest that this current is carried by Na^+ ions through the Ca channels. The Na current decreased in amplitude as the concentration of external divalent cations was elevated. Blocking the Na current by divalent cations could be approximated by a bimolecular interaction between divalent cation and channel, with a dissociation constant of 1.2 μM for Ca^{2+} and 60 μM for Mg^{2+}. Single channel currents were recorded in the cell-attached configuration. With a pipette solution of pCa = 7.5 or pCa > 8, the single channel I–V relationship was linear and the slope conductance was 70–75 pS. For 40 mV depolarizations from the resting potential, unitary currents were smaller at pCa = 6 than at pCa = 7.5. However, single channel events, which were observed after the repolarizing step to the resting potential, were much the same amplitude. The open time histogram was fitted with a single exponential having a time constant of 1.9 ms at around −40 mV (pCa > 8, with 5 μM Bay K 8644 in the bath solution), which was decreased with increasing the Ca^{2+} concentration in the pipette solution. Noise power spectra of patch currents at pCa = 6 revealed a high-frequency component at around 1500 Hz. These results suggest that Ca binding to the sites with a high affinity for Ca^{2+} blocks the Na conductance in Ca channels. Reduction of the unitary current at higher concentrations of Ca^{2+} might be attributed to a rapid block by Ca^{2+}.

Key words: Cardiac cells – Ca channels – Ion selectivity – Na ions

Introduction

In preceding work, we demonstrated that the Ca channel current was not affected by removal of external Na^+ when the intracellular Ca^{2+} of single ventricular cells was controlled by internal dialysis (Matsuda and Noma 1984). This finding suggests that under physiological conditions, Ca channels are not measurably permeable to Na^+ (but see Reuter and Scholz 1977). On the other hand, it has been known that Na^+ ions can carry inward currents through the Ca channel when the external Ca^{2+} is reduced (Rougier et al. 1969; Garnier et al. 1969; Hess and Tsien 1984).

Inward currents carried by monovalent ions through Ca channels have been detected in a variety of tissues other than cardiac fibers and recently several investigators have attempted to clarify how ion selectivity of Ca channels is changed in the absence of external divalent cations: in snail neurones (Kostyuk et al. 1983), in single guinea-pig ventricular cells (Hess and Tsien 1984), in frog skeletal muscle fibers (Almers et al. 1984; Almers and McCleskey 1984) and in mouse lymphocytes (Fukushima and Hagiwara 1985). These results suggest that there are binding sites with a high affinity for Ca^{2+} and that the occupation of this site by Ca^{2+} prevents the permeation of monovalent cations, albeit the location of this site being controversial.

Relatively little is known of the properties of single Na currents through Ca channels and the effects of Ca^{2+} on the Na conductance at the level of single channel (Lansman et al. 1985). Thus, I analyzed the fluctuation of whole cell Na currents and recorded single Na currents in the cell-attached configuration, at different concentrations of Ca^{2+}. The results show that Ca^{2+} inhibits the Na current through the Ca channels by reducing the mean open time. Decrease of the unitary current amplitude was ascribed to fast blocking and unblocking kinetics by Ca^{2+}.

Methods

Single ventricular cells from adult guinea-pigs were obtained by enzymatic dissociation (Matsuda et al. 1982) and recordings of the currents were performed using a heat polished patch electrode in the whole cell and cell-attached configurations (Hamill et al. 1981).

The methods used for the whole cell current recordings were similar to those described elsewhere (Matsuda and Noma 1984). The electrode resistance ranged between 1 and 2 MΩ. The series resistance arising mainly at the patch-electrode tip was compensated by summing a fraction of the converted current signal to the command potential. The compositions of the main external and pipette solutions are listed in Table 1. To minimize currents through the K channels, the pipettes were perfused with a Cs-rich solution and external K^+ was removed. Under this condition, currents in inwardly rectifying K^+ channels are abolished (Matsuda and Noma 1984). A standard Ca-free external solution was prepared by omitting $CaCl_2$ and adding

Offprint requests to: H. Matsuda at the present address
* *Present address:* 2nd Department of Physiology, Faculty of Medicine, Kyushu University, Fukuoka 812, Japan

Table 1. Composition of solutions (mM)

	External						
	NaCl	NaH_2PO_4	KCl	$MgCl_2$	$CaCl_2$	EGTA	HEPES-NaOH
Normal solution	144	0.33	5.4	0.5	1.8	–	5
0 K solution	144	0.33	–	0.5	1.8	–	5
Standard 0 Ca solution[a]	144	0.33	–	2.3	–	0.1	5
0 Mg, low-Ca solution							
pCa = 4.2	144	0.33	–	–	0.2	0.1	5
pCa = 4.6	144	0.33	–	–	0.13	0.1	5
pCa = 5.0	144	0.33	–	–	0.11	0.1	5
pCa = 5.5	144	0.33	–	–	0.102	0.1	5
pCa = 5.9	144	0.33	–	–	0.1	0.102	5
pCa = 6.4	144	0.33	–	–	0.1	0.11	5
pCa = 7.0	144	0.33	–	–	0.1	0.13	5
pCa = 7.5	144	0.33	–	–	0.1	0.2	5
0 Ca, Mg-containing solution[b]							
pMg = 2.3	144	0.33	–	5.0	–	0.1	5
pMg = 2.6	144	0.33	–	2.3	–	0.1	5
pMg = 3.0	144	0.33	–	1.0	–	0.1	5
pMg = 3.3	144	0.33	–	0.5	–	0.1	5
pMg = 4.0	144	0.33	–	0.1	–	0.1	5

Pipette solution for whole cell current recordings

	Cs aspartate	CsCl	$MgCl_2$	EGTA	ATP[c]	HEPES-CsOH
Cs-rich solution	110	20	1	5	5	5

Pipette solution for single channel current recordings

	NaCl	NaH_2PO_4	$CaCl_2$	EGTA	HEPES-NaOH
0 Mg, 0 Ca solution					
pCa > 8	144	0.33	–	2	5
0 Mg, low-Ca solution					
pCa = 6.0	144	0.33	1	1.03	5
pCa = 7.5	144	0.33	1	2	5

External solution contained 5.5 mM glucose and the pH was adjusted to 7.4. In pipette solution for whole cell current recordings, pH was adjusted to 7.3. The liquid junction potential between the internal solution and the normal external solution was corrected (Matsuda and Noma 1984). Pipette solution for single channel current recordings contained 31 μM TTX unless otherwise indicated and the pH was adjusted to 7.4.

[a] Containing 0.5 μM epinephrine

[b] Mg^{2+} and Ca^{2+} concentration was calculated from the apparent dissociation constants (pCa > 8)

[c] Adenosine 5′-triphosphoric acid as dipotassium salt; Sigma

0.1 mM ethyleneglycol-bis(β-aminoethylether)N,N′-tetra-acetic acid (EGTA). It should be noted that the cell membrane becomes leaky in solutions without divalent cations (Kostyuk et al. 1983; Fukushima and Hagiwara 1985). An increase in leakage current developing in Ca-free solution was depressed by adding equimolar Mg^{2+}, which partially depressed the Na current under investigation (see Results). Thus, to obtain a larger Na current, 0.5 μM epinephrine was added in most experiments with 2.3 mM external Mg^{2+}. When the current was compared at different external Ca^{2+} concentrations, external Mg^{2+} was removed. The free Ca^{2+} concentration was measured with a Ca^{2+}-sensitive electrode (Model 93–20, Orion Research) and expressed by its inverse $\log_{10}$. Mg^{2+} solution was prepared by adding a desired concentration of $MgCl_2$ to Ca-free solution containing 0.1 mM EGTA. The Mg^{2+} concentration was calculated from the apparent dissociation constants (Fabiato and Fabiato 1979) and expressed by its inverse $\log_{10}$. Whole cell current and voltage signals were stored on magnetic tape (TEAC, R-210) for computer analysis (Hitachi, E-600). Current traces were displayed without subtraction of leak current or capacitive current. The procedure used to estimate the unit amplitude from the variance-to-mean current relationship is described in the Results

Single channel currents were recorded from cell-attached patches on cells superfused with normal external solution, to which Bay K 8644 was added in most experiments to promote extended opening of the channel. The pipettes (5–10 MΩ resistance) were made from capillaries of high melting temperature glass and were coated with silicone (Shin-etsu Chemical Co.). Records were made with an EPC-5 or EPC-7 patch clamp amplifier (List Electronic).

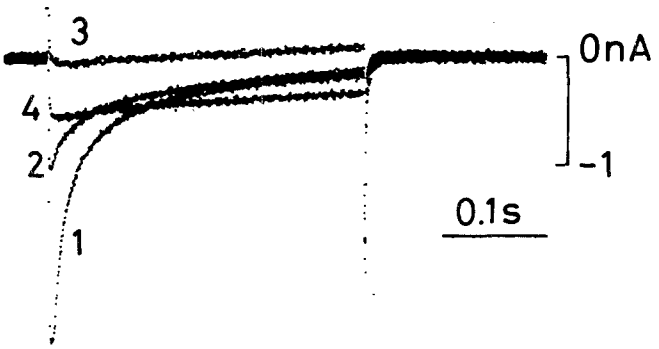

Fig. 1. Change in the Ca channel current after removal of external Ca^{2+}. Depolarizing pulses of 300 ms were applied from −43 to +7 mV every 10 s. Membrane currents before (trace *1*) and 3 min (trace *2*), 5 min (trace *3*) and 10 min (trace *4*) after exchanging K-free external solution for standard Ca-free solution were superposed

Data were stored on magnetic tape (TEAC, R-210) in earlier experiments (Fig. 6) and on a video cassette (Victor, BR6400) using a PCM converter system (NF, RP-880; reproduce bandwidth 10 kHz) in later experiments (Figs. 7–10). Currents were filtered using a four-pole low-pass Bessel filter (NF Circuit Design Block Co. FV-625A, 48 dB/oct) with a 3-dB corner frequency of 1.4 kHz and sampled every 0.2 ms, unless otherwise indicated. To analyze fast flickering kinetics of single channel current recordings, patch current data were low-pass filtered to 3 kHz by a four-pole Butterworth filter and sampled every 0.1 ms. Sampling was begun 10 ms after the start of the 130 ms clamp pulse. Power spectral densities were calculated on 1024 point data sections via a fast Fourier transform routine, resulting in one-sided spectra. Twenty to forty such spectra were averaged. Spectra of background noise sampled from frames without events were subtracted.

Voltage steps were applied every 6 s in whole cell current recordings and every 3–4 s in single channel current recordings, unless otherwise indicated. All experiments were carried out at 35–37°C. Average results throughout this paper are given as mean ± SD.

Results

Development of the inward current in the absence of Ca^{2+}

It is known that removal of external Ca^{2+} induces a biphasic effect on action potential of cardiac preparations; a shortening of the action potential followed by a progressive lengthening (e.g. Rougier et al. 1969). The change in the Ca channel current underlying such an effect was studied, under conditions where the K currents were minimized by removing K^+ from both sides of the membrane (Fig. 1). After K-free external solution containing 1.8 mM $CaCl_2$ was exchanged for standard Ca-free solution, the Ca current (trace 1) decreased gradually (trace 2) and disappeared 5 min later (trace 3). Further exposure to the Ca-free solution induced an inward current which was sustained during the 300 ms clamp pulse (trace 4).

The proposal that the inward current in the absence of external Ca^{2+} is carried through the Ca channels is deduced from the following findings. (1) The inward current was not affected by addition of 3.1 μM TTX to the external solution (not shown). (2) Organic Ca channel blockers such as verapamil or D-600 suppressed this current (Fig. 3). (3) The inward current was increased in amplitude in the presence of 0.5 μM epinephrine by 99 ± 50% (n = 5, figure is not shown).

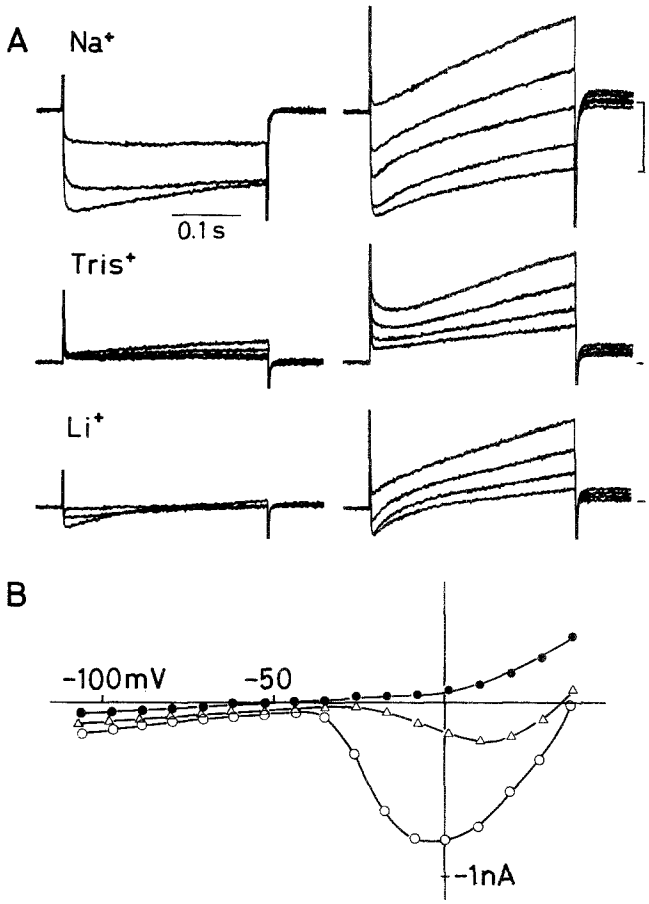

Fig. 2A, B. Membrane currents in Ca-free solutions containing Na^+, $Tris^+$ and Li^+ as the major cation. **A** Total NaCl in standard Ca-free solution (*upper panel*) was replaced with Tris-Cl (*middle panel*) or LiCl (*lower panel*). The pH was adjusted by 5 mM LiOH-HEPES in Li^+ solution and by Tris-Cl buffer (149 mM) without HEPES in $Tris^+$ solution. Traces with Na^+ and $Tris^+$ were obtained during voltage steps to between −26 and +36 mV in 9–10 mV increments, and traces with Li^+ during voltage steps to between −17 and +37 mV in 9–10 mV increments. Holding potential, −43 mV. The marks to the right of each panel indicate zero current. The current calibration represents 0.5 nA. **B** Initial I–V relations with Na^+ (*open circles*), $Tris^+$ (*filled circles*) and Li^+ (*open triangles*)

Na and Li conductance in Ca channels in the absence of Ca^{2+}

Figure 2A shows membrane currents in Ca-free solution containing Na^+, $Tris^+$, or Li^+, as the major cation. The initial currents are plotted against the membrane potential in Fig. 2B (leakage currents are not subtracted). It is evident that Na^+ carries a large inward current while the large organic cation $Tris^+$ does not. Replacing Na^+ with $Tris^+$ unmasked the outward current, which may be attributed to the Cs current, either through a non-specific voltage-dependent conductance (Byerly and Hagiwara 1982; Matsuda and Noma 1984) or through the Ca channel.

After replacing external Na^+ with Li^+, the inward current peaked at a smaller magnitude and at more positive potential than the Na current. The reversal potential of the

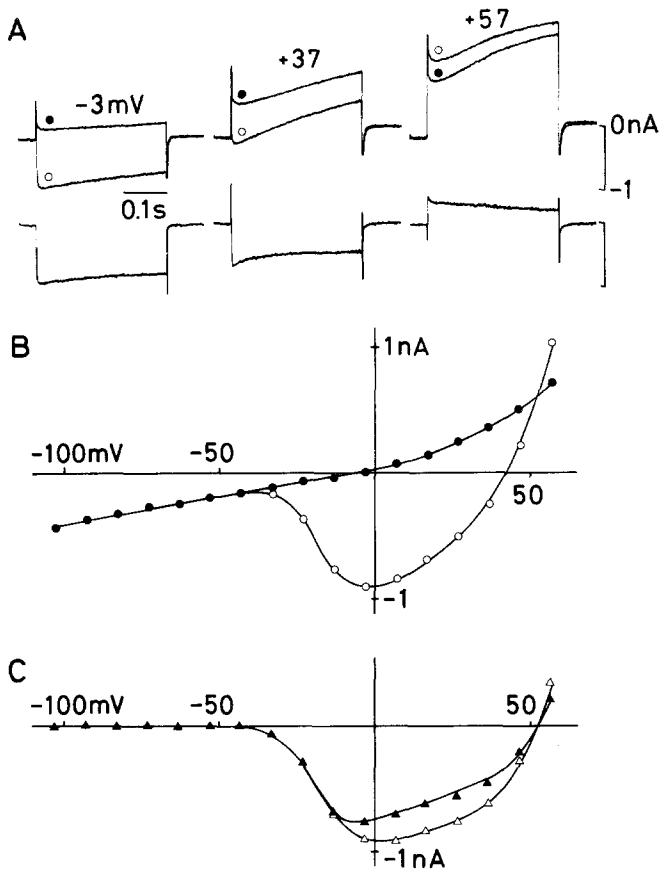

Fig. 3A–C. Isolation of the Na current by D-600. **A** The upper panel shows superimposed current records before (*open circles*) and after (*filled circles*) addition of 1 μM D-600 to standard Ca-free solution. 300 ms step depolarizations from −43 mV to the potentials indicated. The lower panel shows differences between currents before and after D-600 application. **B** Initial currents before (*open circles*) and after (*filled circles*) addition of D-600 are plotted against the membrane potential. **C** Difference currents (*open triangles*, initial; *filled triangles*, late) are plotted against the membrane potential

Li current obtained using D-600 (1 μM) in other cells was more positive by 10–15 mV than that of the Na current. Thus there may be a difference in screening effects between Na^+ and Li^+. The current amplitude was measured at the potential that gave the largest inward current after subtraction of linear leakage currents (see below). It decreased to 30 ± 6% (n = 3) of the control Na current after substitution of Li^+ for total Na^+, suggesting that Li^+ is a weaker charge carrier than Na^+. The channels under investigation seem to be less permeable to Li^+ than the fast Na channel, for which the Li^+:Na^+ permeability ratio is reported to be 0.92 in rat ventricular cells (Akaike et al. 1984), 0.93 in frog nerve (Hille 1972) and 1.1 in the squid axon (Chandler and Meves 1965).

Isolation of the Ca channel current developed in the absence of external Ca^{2+}

In order to isolate the Ca channel current, the current was recorded before (open circles) and after (filled circles) application of 1 μM D-600 (upper panel of Fig. 3A) and the Ca blocker-sensitive current (difference current) was obtained by subtracting the current after the drug application from that before the application (lower panel of Fig. 3A). The resulting current reversed between +37 mV and +57 mV, and currents in both directions were inactivated slowly during the depolarizing pulse. The difference current at +37 mV decayed more slowly than the current before subtraction, indicating that the time-dependent current change during larger depolarizations results partly from activation of a non-specific time- and voltage-dependent outward current.

In Fig. 3B, the initial current before (open circles) and after (filled circles) application of D-600 was plotted against the membrane potential. The current-voltage (I–V) curves after application of the drug were almost linear up to around +10 mV. This validates assessing the current amplitude as the difference between the point on the I–V curve and the point on the straight line extrapolated from the hyperpolarizing region (manual subtraction of linear leakage currents).

In Fig. 3C the initial amplitude (open triangles) and amplitude near the end of the 300 ms clamp pulse (filled triangles) of the difference current have been plotted against the membrane potential. Both the initial and late current reverse at around +50 mV. Essentially the same results were obtained in four other experiments and the reversal potential averaged 46 ± 6 mV (n = 5). This is in contrast to the case of the Ca current, where the late current reverses at a potential 10–20 mV less positive than the initial current (Matsuda and Noma 1984). (The reversal potential of the initial current was 76 ± 5 mV, n = 10.) The above result suggests that the reversal of the D-600 sensitive Na current is a true reversal of the Ca channel current.

If Na^+ is assumed to be the only charge carrier, the averaged reversal potential of +46 mV would mean that the intracellular Na^+ concentration is 25.4 mM. Such a high intracellular Na^+ concentration is unlikely because the pipette solution did not contain Na^+ and the fast Na current reversed around +100 mV. Under the condition where the Ca channels become permeable to Na^+, Cs^+ is likely to be permeant, and the less positive reversal potential than that of the fast Na current may be attributable to the outward Cs movement through the Ca channels.

As described below, the Na current in Mg-free, low-Ca solution peaked at a potential 20–30 mV more negative than the original Ca current. This is ascribed to surface potential changes caused by reducing divalent cations in the external solution (McLaughlin et al. 1971). The degree of the negative shift of the peak inward current was decreased in standard Ca-free solution (Fig. 3C). The reversal potential of the Na current is more positive in standard Ca-free solution than in Mg-free, low-Ca solution. (The reversal potential in Mg-free solution predicted from the single channel I–V curves is +10 mV, see Fig. 7C.) Therefore the positive shift of the potential that gave the largest Na current in standard Ca-free solution is ascribed to surface potential changes caused by increasing Mg^{2+}, rather than alteration of the activation kinetics.

Depressive effect of divalent cations on the Na current

The findings described above favor the view that the Na current developed in Ca-free solution is carried through Ca channels, the ion selectivity and inactivation process of which are modified by removal of external Ca^{2+}. To clarify the mechanism of modification of the Ca channels, I studied the dependence of the amplitude of the Na current on the

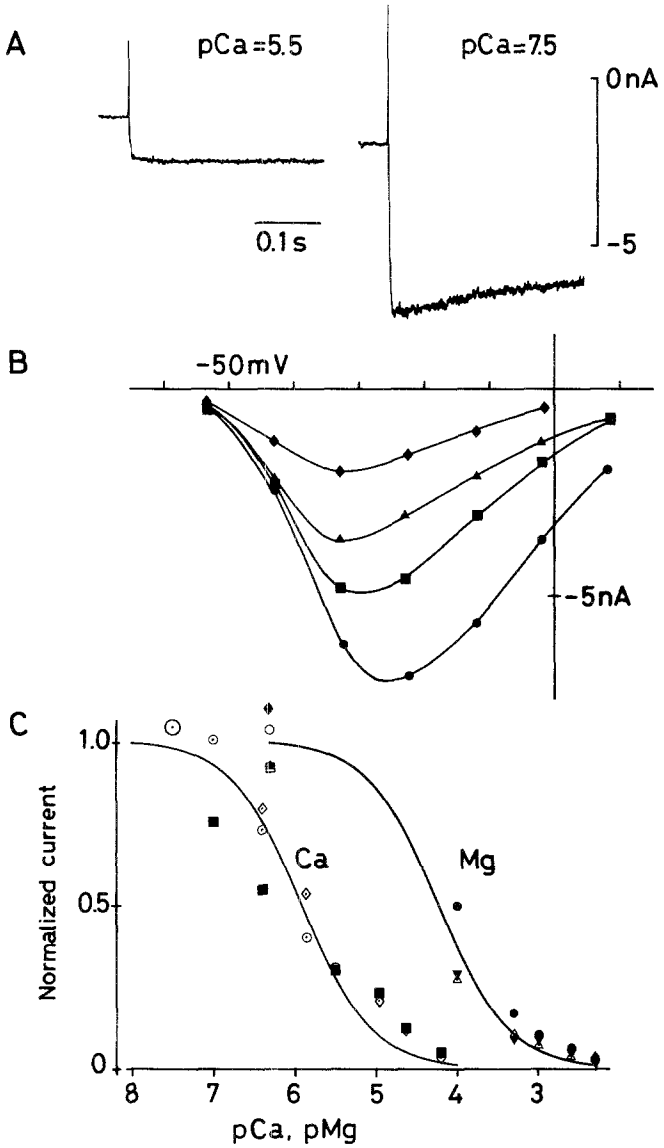

Fig. 4A–C. Depression of the Na current by external Ca^{2+}. **A** The current records at pCa = 5.5 and pCa = 7.5 during steps from a holding potential of −63 mV to −33 mV. **B** I–V relations after leakage currents were subtracted manually. pCa = 5.5 (*diamonds*), 6.4 (*triangles*), 7 (*squares*) and 7.5 (*circles*). **C** Dose-response curve for blockade of the Na current by Ca^{2+} and Mg^{2+}. Currents were measured at the potential that gave the largest inward current at each concentration and expressed as the fraction of the current at pCa = 7.5 (*large open circle*) in cases of Ca^{2+} and as the fraction of the original Ca current in cases of Mg^{2+}. The data from the same cells were presented by the same symbol. The curves which give the best fit to the data points were determined by the least squares method with the assumption that the Na current through the Ca channel is blocked by one Ca^{2+} or by one Mg^{2+} per channel. The dissociation constant is 1.2 μM for Ca^{2+} and 60 μM for Mg^{2+}. Current amplitude was normalized as maximum current to be 1. Maximum current in cases of Mg^{2+} was obtained in Mg-free, low-Ca solution (pCa = 7.5). In this figure, data were plotted assuming that nominally Mg-free solution contained 0.5 μM free Mg^{2+}

extracellular Ca^{2+} or Mg^{2+}. In these experiments, the concentration of Ca^{2+} or Mg^{2+} was lowered stepwise and the I–V relation was measured at each concentration after the new steady state had been reached. The membrane was held at −63 mV in Mg-free, low-Ca solution and at −43 mV in Ca-free, Mg-containing solution. Figure 4A shows the current traces recorded at pCa = 5.5 and pCa = 7.5 during steps from a holding potential of −63 mV to −33 mV. As the external Ca^{2+} was reduced, the Na current was increased in amplitude and was accompanied by fluctuations. The peak amplitude of the Na current at pCa = 7.5 is greater than that of the original Ca current by a factor of 5 (5.03 ± 0.47, $n = 4$).

The peak inward current was plotted against the membrane potential after subtraction of the linear leakage current. Figure 4B illustrates the I–V relations measured in the same cell as in Fig. 4A at pCa = 5.5 (diamonds), pCa = 6.4 (triangles), pCa = 7 (squares) and pCa = 7.5 (circles). The membrane potential giving the maximum peak inward current shifted to the negative direction by 20–30 mV, when the external Mg^{2+} was removed and the external Ca^{2+} concentration decreased from 1.8 mM to pCa = 5. With further decrease of Ca^{2+} from pCa = 5 to pCa = 7.5, there was a slight shift of less than 10 mV, the direction of which was not constant. In Ca-free solution containing 0.1 mM $MgCl_2$ and 0.1 mM EGTA, the peak potential of the Na current was more negative by 10–20 mV than that of the original Ca current. The degree of the negative shift was decreased with increasing external Mg^{2+} from 0.1 to 5.0 mM.

To examine the voltage-dependency of the depressive effect of Ca^{2+} on the Na current, the ratio of the current amplitude to that with the lowest divalent concentration at the same membrane potential was calculated, but no consistent results could be obtained. For example, in the case illustrated in Fig. 4A and B, the depression increased as the membrane potential became positive. In another case, a U-shaped voltage dependence of relative amplitude was detected at lower Ca^{2+} concentrations (pCa > 6) as reported by Fukushima and Hagiwara (1985), and there was no voltage dependency at pCa = 5.

Current amplitude was measured at the potential that gave the largest inward current at each concentration and expressed as the fraction of that at pCa = 7.5 in cases of Ca^{2+} and as the fraction of that in K-free, 1.8 mM Ca solution in cases of Mg^{2+}. The relative amplitude was plotted against the Ca^{2+} or Mg^{2+} concentration in Fig. 4C. The curves which give the best fit to the data points were determined by the least squares method with the assumption that the Na current is blocked by one or two Ca^{2+} ions per channel. The one-to-one binding curve fits the data points better than the one-to-two binding curve, and so only one-to-one binding curves are illustrated in Fig. 4C. The dissociation constant is 1.2 μM for Ca^{2+}. Although there are a few data points at pMg > 4, the data points for Mg^{2+} could be fitted by the one-to-one binding curve, with a dissociation constant of 60 μM. Thus, the depression of the Na current by Mg^{2+} was one-fiftieth of that by Ca^{2+}.

Unit amplitude and total number of channels determined by noise analysis

The amplitude of the macroscopic current depends on three factors: the number of functional channels (N), the probability that an individual channel is open (p), and the current carried by an open channel (i). To know which of these factors decreases with increasing external Ca^{2+}, I analyzed current fluctuations developing at lower Ca^{2+} concentrations.

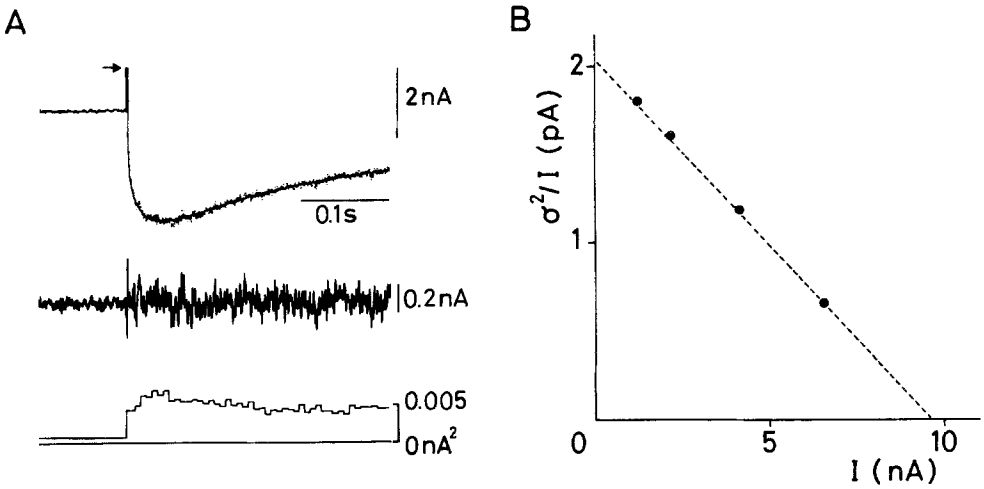

Fig. 5A, B. Measurement of single channel current. **A** Na current in response to depolarizations from −63 to −41 mV at pCa = 6.4 (*plotted by point*) shows current fluctuations during clamp pulses around the mean time course of the current (*plotted by line; upper trace*). The middle trace shows the residual fluctuations obtained by subtracting the mean time course of the current, which were made for individual currents by shifting vertically the average current, derived from all or half of fifty successive records, so that the variance of the residual fluctuations would be minimized. This procedure prevented error caused by slight long-term drifts in the current amplitude. Variance of the residual fluctuations was calculated for each sampling point and averaged for consecutive 15 sampling points during the depolarizing pulse and for consecutive 250 points at the holding potential. The bottom trace is the average variance from 43 sweeps. Membrane currents were fed via a four-pole Butterworth filter with a cut-off frequency of 1 kHz to a computer and digitized with a sampling interval of 0.4 ms. The arrow indicates the leakage current amplitude. **B** The variance-to-mean current relationship. Mean variance was obtained by averaging over about 300 successive time points in the middle of clamp pulses and subtracting the variance associated with the holding current. The peak amplitude of the average current was used for the mean current (I) after subtraction of the linear leakage current. Mean variance and mean current obtained at different voltage steps spaced 2−3 mV apart were plotted. From an intersection of Y-axis and from a slope of a straight line, a single channel current amplitude of 2.04 pA (around −40 mV) and channel number of 4700 per cell were calculated

The variance of current fluctuations (σ^2) is a function of the mean amplitude of the current (I), the unit amplitude (i) and the total number of channels (N), according to the following equation:

$$\sigma^2 = i \cdot I - (I^2/N)$$

where $I = N \cdot i \cdot p$.

To measure the unit amplitude of the Na current from the variance-to-mean current relationship (Sigworth 1980), fifty consecutive current records were obtained with a constant 300-ms voltage step from −63 to −41 mV every 6 s. After the mean time course of the current had been subtracted, the variance of the residual fluctuations was calculated (Fig. 5A). The mean variance increased slightly during the initial 50 ms and then decreased corresponding to the slight inactivation of the current (Fig. 3A). However, these changes are so small that variance-mean plots are not useful for estimating the unit amplitude. Thus, the same procedure was repeated at other voltage steps to −46, −43, and −38 mV. Even such a small change in the voltage step size caused fairly large current changes because of sharp voltage dependence of the current activation. The reversal potential of the Na current in Mg-free, low-Ca solution predicted from the single I−V relations is +10 mV (Fig. 7C). Therefore, difference in the driving force is less than 8% among these test potentials, and so variation in the unit amplitude was neglected. The variance was averaged over about 300 successive time points in the middle of clamp pulses, and the variance associated with the holding current was subtracted. The peak amplitude of the average current was used for the mean current (I) after subtraction of the linear leakage current. Then variance-mean plots were applied, as shown in Fig. 5B. The plot of σ^2/I versus I yields a straight line that intersects the Y-axis at i = 2.04 pA (at pCa = 6.4, around −40 mV) and that has a slope equal to $-1/N$ (N = 4700).

To repeat the constant clamp pulses at each Ca^{2+} concentration was so time-consuming that the experiment was frequently interrupted by deterioration of the cell and I could determine the single channel current at only one Ca^{2+} concentration, in each cell; i = 1.15 pA and N = 4400 at pCa = 5.5, i = 0.87 pA and N = 5600 at pCa = 5.5, and i = 1.38 pA and N = 4800 at pCa = 5.9. These results suggest that it is not the number of functional channels, but rather the single channel current that is decreased with an increase of Ca^{2+}.

Single Na current through the Ca channel

Single Ca channel currents, with Na^+ as charge carriers, were recorded from cell-attached membrane patches using the pipette filled with the solution containing 144 mM NaCl and buffered at pCa = 6, pCa = 7.5 and pCa > 8. Depolarization of the patch membrane from the resting membrane potential (RP; around −80 mV in normal external solution; see Matsuda and Noma 1984) induced inward-going channel currents characterized by a short life time (less than 2 ms) and clustering of the channel openings, as shown in Fig. 6A (pCa = 7.5) and B (pCa = 6). That this current is different from the Na channel current is evident from the following findings: (1) the current was induced in the presence of TTX in the pipette solution, but was suppressed by adding 1 μM D-600 to the bathing solution (not shown) and (2) the averaged current was inactivated little during 130 ms depolarizing pulse (Fig. 6C).

In accordance with results of noise analysis of the whole cell currents, unitary current amplitude at pCa = 7.5

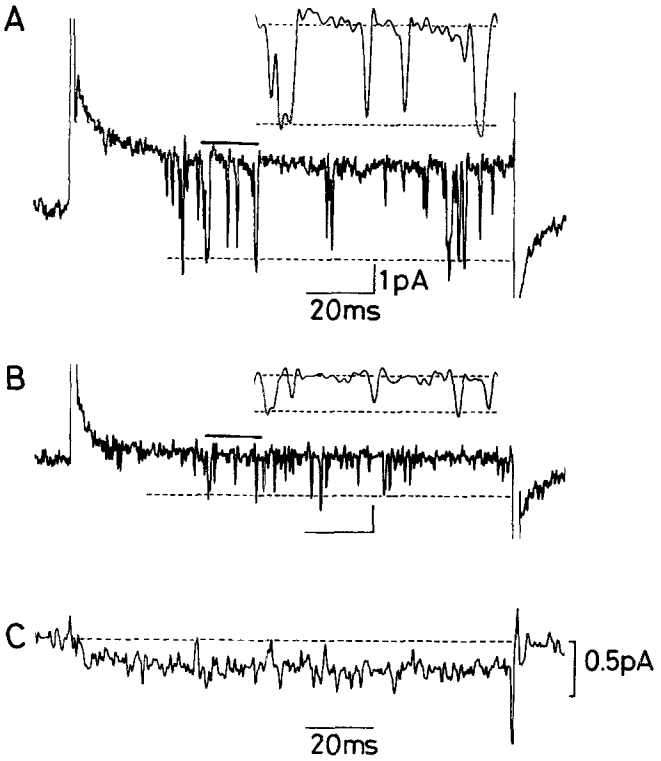

Fig. 6 A – C. Single channel currents recorded in the cell-attached confifurations. **A, B** Current responses to 40 mV voltage steps from a resting potential of around −80 mV (leakage and capacitive currents are not subtracted). Pipette solution contained 63 μM TTX and was buffered at pCa = 7.5 (A) and pCa = 6 (B). Currents were low-pass filtered with a cut-off frequency of 1.2 kHz (−3 dB) and sampled every 0.2 ms. The inset shows an expansion (by four times) of the part marked by the solid line. Unitary current amplitude and baseline level (in inset) are indicated by the dotted line. The cell was superfused with normal external solution. **C** Average current from the data in B. Fifty current sweeps were averaged after subtraction of leakage and capacitive currents. Zero current level is indicated by the dotted line

seemed larger than that at pCa = 6. The unit amplitude was measured from events which showed clear levels of open channel currents, though such events were not so frequent at pCa = 6. Average amplitude during depolarizing clamp steps of 40 mV from the resting potential is 3.30 ± 0.13 pA at pCa = 7.5 (five patches) and 1.44 ± 0.06 pA at pCa = 6 (six patches). However, if Ca^{2+} and Na^{+} compete for permeation through the Ca channel and blocking kinetics by Ca^{2+} is too fast to be detected, the unitary current amplitude might be reduced. Expecting that discrete blocking events were revealed by Bay K 8644, which has been reported to prolong the mean open time without affecting the unitary current amplitude (e.g. Hess et al. 1984), I added the drug to the bathing solution at a concentration of 5 μM and studied the effect of Ca^{2+} on single Na currents.

The properties of single Na current through Ca channels recorded under the minimum influence of Ca^{2+} will be described briefly, and then the effect of Ca^{2+} will be described. The Ca-free (2 mM EGTA) solution containing 144 mM NaCl (pCa > 8) was used to minimize the effect of Ca^{2+}. Figure 7A shows voltage dependence of single Na current through Ca channels. Membrane potential was stepped by the indicated step size from the resting potential. Ca channels switch randomly between open and closed states, and do not dwell at a constant level during channel openings. As a result, a probability density histogram of the patch current obtained for the current traces in Fig. 7A showed a rather obtuse peak at the open current level compared to a sharp peak around zero current (Fig. 7B). Thus I decided to estimate the amplitude of unitary current simply by eye. The level of single channel currents is indicated by a dotted line on each trace in Fig. 7A, except for the bottom trace where no obvious events are observed. This level is indicated also in Fig. 7B by an arrow head. The current amplitude was plotted against voltage in Fig. 7C. I–V relationship is approximately ohmic with a slope conductance of about 70 pS. The reversal potential predicted from the I–V curve is +10 mV (RP + 90 mV), though I did not apply depolarizing pulses larger than 100 mV and could not observe the outward current.

To analyze the kinetic characteristics, open time and closed time histograms were constructed (Fig. 8). The threshold for openings was set at about one-third the amplitude of the openings studied (inset). The open time histogram (Fig. 8A) was described by a single exponential function with a time constant (τ_o) of 1.89 ms (during depolarization of 40 mV). Neglecting a few events of the closed time longer than 10 ms, the closed time histogram was described by a single exponential function with a time constant (τ_c) of 1.59 ms (Fig. 8B). This represents the mean duration of the short gaps during bursts. If a burst is defined as any series of openings interrupted only by gaps shorter than 4.5 ms ($= 4 \times \tau_c$ at pCa = 6, see below; Sakmann and Trube 1984), histograms of the burst durations and the gap durations were fitted by a single exponential function. In this case, the time constant fit for the histogram of the burst durations (the mean burst length) was 28.7 ms and the time constant fit for the histogram of the gap durations longer than 4.5 ms (the mean closed time between bursts) was 10.1 ms (not shown).

Figure 9 shows the current traces recorded from four different cells with pipette solution buffered at pCa = 7.5 (Fig. 9A) and pCa = 6 (Fig. 9B). Also in the presence of Bay K 8644, single channel currents at pCa = 6 appeared smaller than that at pCa = 7.5 during 40 mV depolarization from the resting potential. Currents after the repolarizing voltage step to the resting potential, however, had nearly the same amplitude. The current amplitude at the resting potential at pCa = 6 averaged 6.30 ± 0.46 pA (10 patches), which was plotted by open symbol in Fig. 7C. This result can be explained by assuming that the blocking effect of Ca^{2+} is voltage dependent and that repolarization relieves it. The slope conductance measured at pCa = 7.5, 70–75 pS, was much the same with that at pCa > 8 (Fig. 7C).

Kinetic characteristics of single Na currents through Ca channels measured during 40 mV depolarization at different Ca^{2+} concentrations are summarized in Table 2. τ_o is remarkably decreased at pCa = 6. τ_c and the burst length are also decreased, but to a lesser extent.

To analyze the fast kinetics of single channel current recordings, power density spectra of patch current fluctuations were calculated using a fast Fourier transform routine. Figure 10 shows a typical example obtained at pCa > 8 and pCa = 6, during 40 mV depolarization from the resting potential. The data at pCa > 8 were fitted well with the double Lorentzian function. The time constants associated with the low-frequency corner and the high-frequency corner are 0.82 ms and 0.16 ms, respectively. The former corresponds

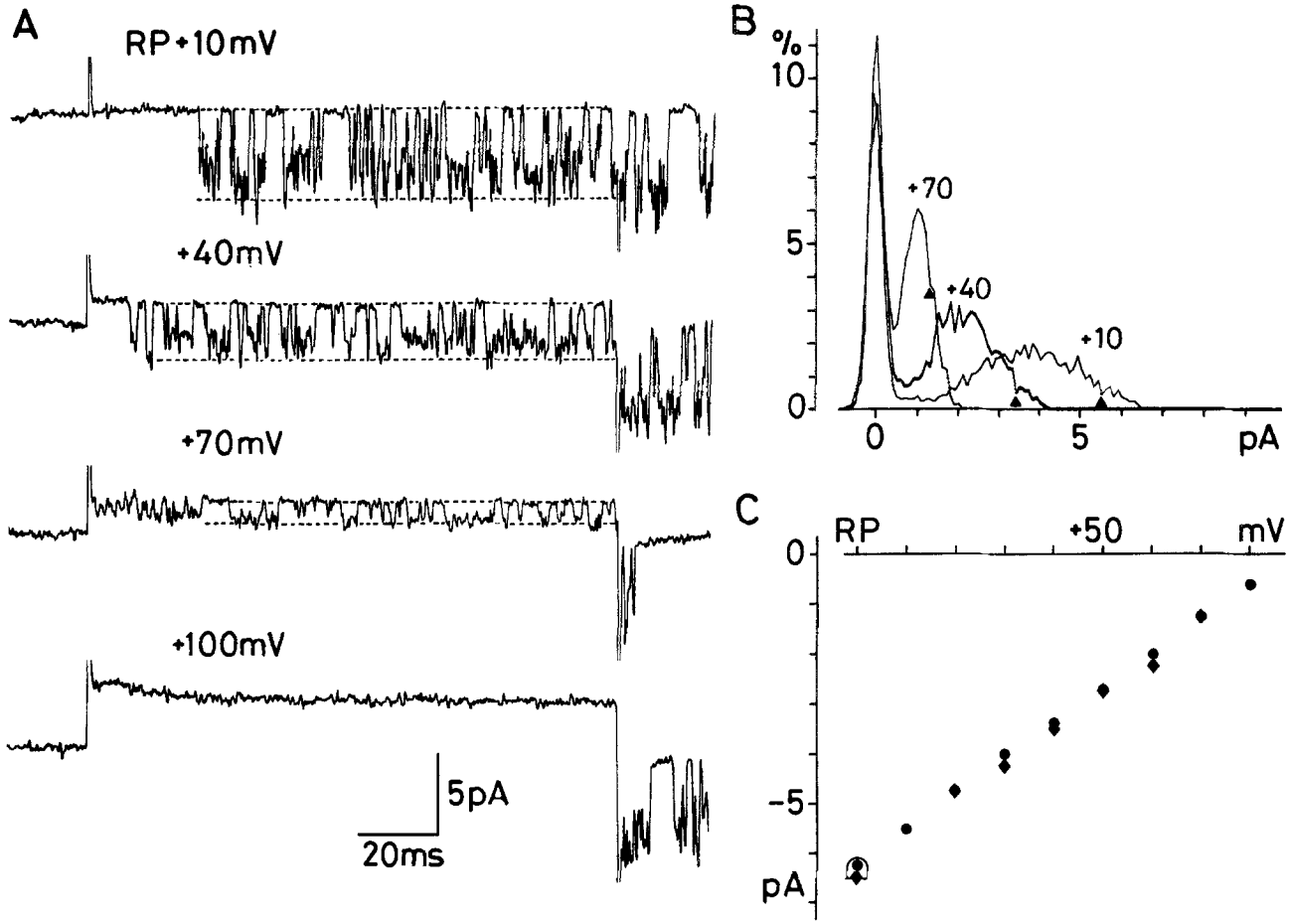

Fig. 7 A – C. Voltage dependence of single Na currents through Ca channels. **A** Records in response to 130 ms depolarizing pulse. Membrane potential was stepped by the indicated step size from the resting potential (RP, about −80 mV). The capacitive transient was reduced by analog compensation. Single channel current amplitude and baseline level are indicated by the dotted line. Ca-free pipette solution (pCa > 8). Bath solution contained 5 μM Bay K 8644. **B** Amplitude histogram obtained for the current traces in A. It showed an obtuse peak at the open channel level and the amplitude of single channel current was determined by eye (*arrow head*). **C** Single channel I – V relationships obtained from the same patch as in **A** and **B** (*filled circles*, 70 pS) and from another patch using the pipette solution buffered at pCa = 7.5 (*filled diamonds*, 75 pS). *Open symbol* represents the current amplitude observed at pCa = 6 after the repolarizing voltage step to the resting potential (6.30 ± 0.46 pA, 10 patches)

well with the time constant of 0.86 ms calculated from τ_o and τ_c presented in Fig. 8. The latter may represent the fast flickering kinetics of the single Na current through the Ca channel shown in Fig. 7A and inset of Fig. 8A. Both corner-frequencies showed no obvious potential dependency (212 Hz and 1080 Hz during 20 mV depolarization, 164 Hz and 864 Hz during 30 mV depolarization and 200 Hz and 952 Hz during 50 mV depolarization). The same result was obtained in two other patches.

A slow component below 50 Hz was revealed in the spectra at pCa = 6. This might be ascribed to gating activities of bursts, because the burst length and closed time between bursts at pCa = 6 were 18 ms and 10 ms, respectively (Table 2). The solid line in the spectra at pCa = 6 was the best fit obtained by applying single Lorentzian function to the data between 400 and 3000 Hz. The corner-frequency was 1584 Hz in this case and the time constant associated with the averaged corner-frequency (1505 ± 95 Hz, 5 patches) is 0.10 ms.

Discussion

In cardiac cells, the Na current in the absence of external Ca^{2+} decays much more slowly than the Ca current. This is in contrast to the monovalent currents through Ca channels in other excitable cells, which show a similar decay time course to the Ca current (Kostyuk et al. 1983; Almers and McCleskey 1984). Nevertheless, the suppression by Ca channel blockers (Rougier et al. 1969; Garnier et al. 1969) and augmentation by epinephrine (in this work) strongly suggest that the cardiac Na current is also carried through Ca channels. The slow inactivation of Ca channels after Ca chelation suggests that the major inactivation mechanism of the Ca channel is not operating when Na^+ is the charge carrier. This is consistent with the view that inactivation of the Ca channel results from Ca entering upon depolarization rather than from the membrane potential effects alone (Ca-mediated inactivation of the Ca conductance: e.g. Eckert and Tillotson 1981; in the cardiac fibers, Mentrard et al. 1984; Kokubun and Irisawa 1984; Lee et al. 1985).

Another difference is that the cardiac Ca channel is less permeable to Li^+ than to Na^+. The Ca channels, under conditions of reduced external Ca^{2+} concentrations, are reported to be equally permeable to Li^+ and Na^+: in molluscan neurones the $Li^+ : Na^+$ permeability ratio is 0.8 (Kostyuk et al. 1983) and, in frog skeletal muscle, it is 1 (Almers et al. 1984). However, in cardiac cells, Li^+ cannot carry such a large inward current as Na^+ (Chesnais et al. 1975; Lansman et al. 1985). In the present study, the

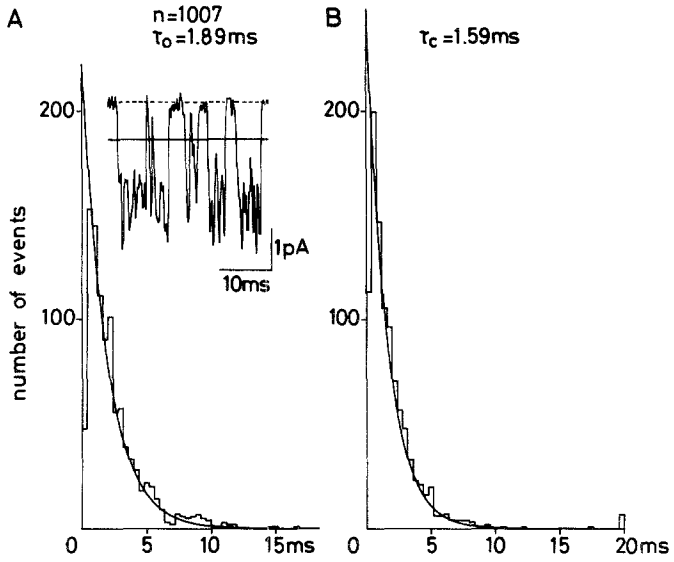

Fig. 8. Distribution of open time (**A**) and closed time (**B**) at pCa > 8 during 40 mV depolarization from the resting potential. The same patch and series of records as in Fig. 7. A threshold level for discrimination of open and closed states was set at around one-third of the open level, as shown by the *solid line in the inset*. The dotted line indicates the baseline level. The open time histogram formed in 0.4 ms bins was fitted with a single exponential function with a time constant of 1.89 ms (**A**). The closed time histogram was constructed with 0.4 ms bins and fitted with a single exponential function with a time constant of 1.59 ms, neglecting a few events of the closed time longer than 10 ms (**B**). Bath solution contained 5 μM Bay K 8644

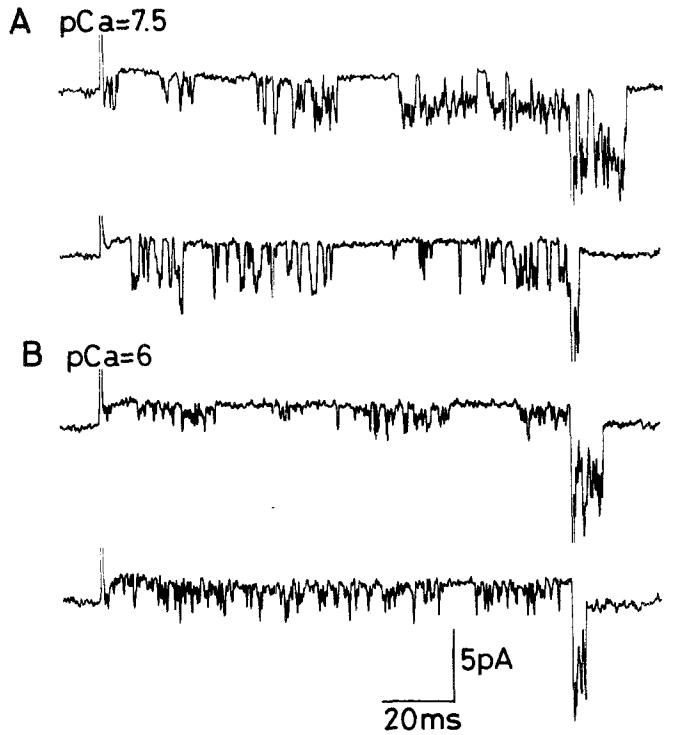

Fig. 9 A, B. Voltage-dependent block by Ca^{2+} of single Na currents through Ca channels. Each record was obtained from different patches, using the pipette solution indicated. Bath solution contained 5 μM Bay K 8644. Single channel currents at pCa = 6 appeared at a less magnitude and a shorter duration than at pCa = 7.5 during 40 mV depolarization from the resting potential. However, currents after the repolarizing voltage step to the resting potential are much the same amplitude as that at pCa = 7.5

Table 2. Kinetic characteristics of single Na currents through Ca channels during 40 mV depolarization at different Ca^{2+} concentrations

	pCa > 8	pCa = 7.5	pCa = 6
Open time (τ_o; ms)	1.94 ± 0.31	1.48 ± 0.11	0.26 ± 0.05
Closed time within bursts (τ_c; ms)	1.52 ± 0.07	1.44 ± 0.12	1.17 ± 0.17
Burst length (ms)	26.5 ± 3.3	24.9 ± 1.5	18.3 ± 1.2
Closed time between bursts (ms)	9.7 ± 1.3	12.3 ± 6.0	10.0 ± 3.5

Analysis was done in patches containing one active channel (three patches at pCa > 8 and pCa = 7.5 and six patches at pCa = 6). A burst was defined as any series of openings interrupted only gaps shorter than 4.5 ms (= $4 \times \tau_c$ at pCa = 6; Sakmann and Trube 1984)

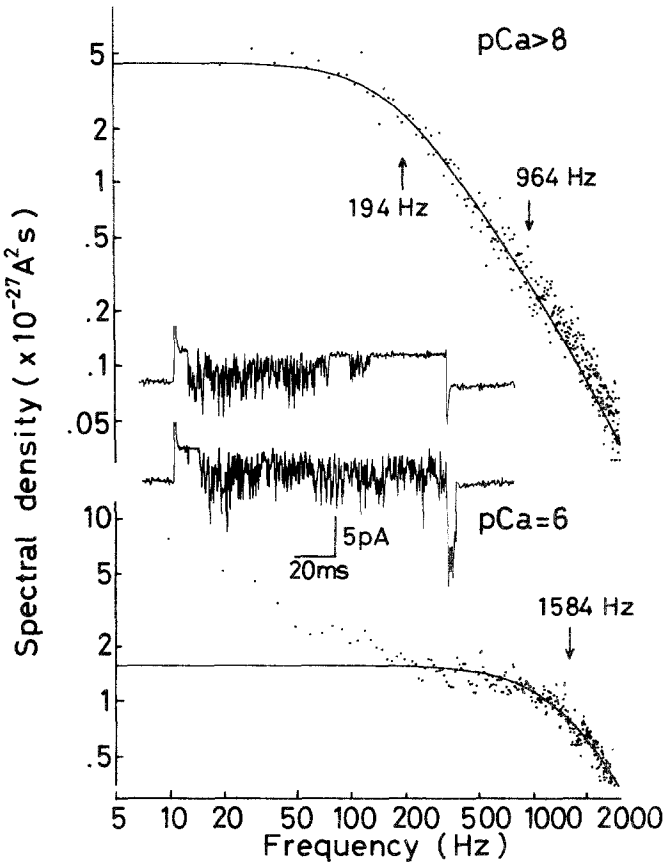

Fig. 10. Power density spectra of patch current fluctuations measured during 40 mV depolarization from the resting membrane potential. Bath solution contained 5 μM Bay K 8644. The spectra at pCa > 8 fitted well with the double Lorentzian function. The corner-frequencies of slow and fast component, 194 and 964 Hz, are indicated by *arrows*. The zero frequency asymptotes of the slow and fast components were 4.16×10^{-27} and 2.10×10^{-28} A^2 s, respectively. The same patch as in Fig. 7 and 8. The spectra at pCa = 6 was obtained from patch containing several active channels (inset). The solid line was the best fit obtained by applying single Lorentzian function to the data between 400 and 3000 Hz. The corner-frequency was 1584 Hz and the zero-frequency asymptote was 1.56×10^{-27} A^2 s. The slow component below 50 Hz of power density spectra was ascribed to the bursting activities of the channels

amplitude of the Ca channel current decreased to 30% after total replacement of the external Na^+ with Li^+ (Fig. 2). Such a diminished permeability of the Ca channel to Li^+ than to Na^+ was observed also in case of gastrointestinal smooth muscle (Prosser et al. 1977) and uterine smooth muscle (Mironneau et al. 1982), where the prolonged action potential induced by Ca chelation disappeared after replacing Na^+ with Li^+.

Despite these differences, the Na current is depressed by Ca^{2+} of a micromolar level as is the case in other excitable cells. Hess and Tsien reported that 1.3 μM external Ca^{2+} lower the Na influx through the Ca channel to $33 \pm 4\%$ in single ventricular cells of guinea-pig (1984). In the present work, it was shown that depression of the Na current by external divalent cations can be described by a bimolecular interaction between a single ion and channel. The dissociation constant of 1.2 μM for Ca^{2+} and 60 μM for Mg^{2+} agrees well with the result of Hess and Tsien (1984) and with those obtained in other excitable cells: 0.3 μM and 60 μM in Helix neurones (Kostyuk et al. 1983), 2 μM and 30 μM in mouse lymphocytes (Fukushima and Hagiwara 1985) and 0.7 μM for Ca^{2+} in frog skeletal muscle (Almers et al. 1984).

Prevention of Na movements through the Ca channel by micromolar level of Ca^{2+} has been attributed to a binding site with a high affinity for Ca^{2+} which regulates the ion selectivity of the Ca channels (Kostyuk et al. 1983). When Ca chelation makes this site free, the Ca channel acquires a permeability to Na^+ that is not present at physiological Ca^{2+} concentrations.

There is no direct evidence as to where such a Ca-binding site locates. From the finding that reduction in the Na current by Ca^{2+} is not voltage-dependent, Kostyuk et al. (1983) concluded that this high-affinity Ca-binding site is located near the external surface of the membrane and that Ca binding to this site causes conformational changes in the ion-selecting filter. On the other hand, Hess and Tsien (1984) and Almers and McCleskey (1984) assumed two high affinity sites within the channel, thereby applying to the Ca channel the multi-ion single-file pore model described by Hille and Schwarz (1978) for the K channels. Their model can account for competitive interaction between Ca^{2+} and Ba^{2+} (anomalous mole fraction effect) as well as the prevention of Na permeation by micromolar level of Ca^{2+}. In the present work, no consistent results could be obtained on the voltage-dependency of the depressive effect of Ca^{2+} in the whole cell clamp experiments. However, unitary currents during 40 mV depolarization were smaller at pCa = 6 than at pCa = 7.5 or pCa > 8 and currents after repolarizing step to the resting potential had nearly the same amplitude. This finding can be interpreted that upon repolarization the Ca bound to the site within the channel enters the interior of the cell to relieve the block, thereby favoring location of a binding site in the channel.

The noise analysis of single channel currents at pCa = 6 revealed a high-frequency component at around 1500 Hz, indicating fast blocking kinetics. Therefore, a decrease in the single channel current amplitude at pCa = 6 is most likely to be an apparent decrease attributed to a rapid block (Yellen 1984). If we assume that the block is a first order process, a simple open ion channel block can be described as:

$$\text{closed}_2 \rightleftharpoons \text{closed}_1 \underset{\alpha}{\overset{\beta}{\rightleftharpoons}} \text{open} \underset{k_{-B}}{\overset{k_{+B}}{\rightleftharpoons}} \text{blocked}.$$

In this situation, there are two ways out of the open state (closing or blocking) with transition rates α and $k_{+B} \cdot (Ca^{2+})_p$, respectively, where $(Ca^{2+})_p$ is the Ca concentration of the pipette solution. Thus, the mean open life time is given $1/[\alpha + k_{+B} \cdot (Ca^{2+})_p]$ (Colquhoun and Hawkes 1983). Because the blocking effect of Ca^{2+} is not expected at pCa > 8, we can obtain the approximate value of α, 526 s^{-1}, from the relation of τ_o (1.9 ms, at pCa > 8) = $1/\alpha$. Using this and τ_o at pCa = 7.5 (1.5 ms) and pCa = 6 (0.26 ms), we can obtain the blocking rate of 141 s^{-1} at pCa = 7.5 and 3320 s^{-1} at pCa = 6. The latter value is smaller than that expected from the linearly proportional relation to the Ca concentration (4460 s^{-1}, see below). However, this discrepancy might be ascribed to an overestimation of τ_o at pCa = 6, because the data were low-pass filtered with a cut-off frequency of 1.4 kHz (−3 dB frequency). From the blocking rate at pCa = 7.5, we can obtain the value of k_{+B} at around −40 mV, 4.46×10^9 M^{-1} s^{-1}. Using the dissociation constant (K_B) at around −30 mV obtained from the whole cell current recordings (Fig. 4), k_{-B}, 5352 s^{-1} was calculated from the relation $K_B = k_{-B}/k_{+B}$. Because the closing rate α and opening rate β, which are estimated from τ_o and τ_c at pCa > 8, are about one order of magnitude smaller than unblocking rate k_{-B} and blocking rate at pCa = 6, we can calculate an approximate time constant of spontaneous fluctuations from the equilibrium between blocking and unblocking of the Na current as $1/[k_{-B} + k_{+B} \cdot (Ca^{2+})_p]$. The resulting value (0.10 ms) is identical to that obtained from noise analysis.

At pCa > 8, the current level of open channels shows flickering. Noise analysis reveals that a fast incomplete closing and opening kinetics with a corner frequency around 1 kHz operates in addition to the dominant slower gating kinetics. The fast flickering kinetics in Ca channels lacking an apparent voltage dependency has been noted also in chick vestibular hair cells (Ohmori 1984). It is interesting that such fluctuations of the single open channel are not obvious with Li^+ or Ba^{2+} as charge carriers (see Lansman et al. 1985 for Li^+). Some species of ions might block their own passage through the Ca channels.

Acknowledgements. I am grateful to Professors H. Irisawa and A. Noma for pertinent advice and discussion throughout this work, to Dr. M. Kameyama for comments on the manuscript and Dr. B. Garthoff of Bayer AG for providing Bay K 8644. This work was supported in part by grants from the Ministry of Education, Science and Culture of Japan and from the Japan Heart Foundation.

References

Akaike N, Yatani A, Nishi K, Oyama Y, Kuraoka S (1984) Permeability to various cations of the voltage-dependent sodium channel of rat single heart cells. J Pharmacol Exp Ther 228:225–229

Almers W, McCleskey EW (1984) Non-selective conductance in calcium channels of frog muscle: Calcium selectivity in a single-file pore. J Physiol 353:585–608

Almers W, McCleskey EW, Palade PT (1984) A non-selective cation conductance in frog muscle membrane blocked by micromolar external calcium ions. J Physiol 353:565–583

Byerly L, Hagiwara S (1982) Calcium currents in internally perfused nerve cell bodies of *Limnea stagnalis*. J Physiol 322:503–528

Chandler WK, Meves H (1965) Voltage clamp experiments on internally perfused giant axons. J Physiol 180:788–820

Chesnais JM, Coraboeuf E, Sauviat MP, Vassas JM (1975) Sensitivity to H, Li and Mg ions of the slow inward sodium current in frog atrial fibres. J Mol Cell Cardiol 7:627–642

Colquhoun D, Hawkes AG (1983) The principles of the stochastic interpretation of ion-channel mechanisms. In: Sakmann B, Neher E (eds) Single-channel recording, chapt 9. Plenum Press, New York London, p 145

Eckert R, Tillotson DL (1981) Calcium-mediated inactivation of the calcium conductance in caesium-loaded giant neurones of *Aplysia californica*. J Physiol 314:265–280.

Fabiato A, Fabiato F (1979) Calculator programs for computing the composition of the solutions containing multiple metals and ligands used for experiments in skinned muscle cells. J Physiol (Paris) 75:463–505

Fukushima Y, Hagiwara S (1985) Currents carried by monovalent cations through calcium channels in mouse neoplastic B lymphocytes. J Physiol 358:255–284

Garnier D, Rougier O, Gargouil YM, Coraboeuf E (1969) Electrophysiological analysis of myocard membrane properties during the plateau of the action potential, existence of a slow inward current in solutions without divalent ions. Pflügers Arch 313:321–342

Hamill OP, Marty A, Neher E, Sakmann B, Sigworth FJ (1981) Improved patch-clamp techniques for high-resolution current recording from cells and cell-free membrane patches. Pflügers Arch 391:85–100

Hess P, Tsien RW (1984) Mechanism of ion permeation through calcium channels. Nature 309:453–456

Hess P, Lansman JB, Tsien RW (1984) Different modes of Ca channel gating behaviour favoured by dihydropyridine Ca agonists and antagonists. Nature 311:538–544

Hille B (1972) The permeability of the sodium channel to metal cations in myelinated nerve. J Gen Physiol 59:637–658

Hille B, Schwarz W (1978) Potassium channels as multi-ion single-file pores. J Gen Physiol 72:409–442

Kokubun S, Irisawa H (1984) Effects of various intracellular Ca ion concentrations on the calcium current of guinea-pig single ventricular cells. Jpn J Physiol 34:599–611

Kostyuk PG, Mironov SL, Shuba YM (1983) Two ion-selecting filters in the calcium channel of the somatic membrane of mollusc neurons. J Membr Biol 76:83–93

Lansman JB, Hess P, Tsien RW (1985) Direct measurement of entry and exit rates for calcium ions in single calcium channels. Biophys J 47:67a

Lee KS, Marban E, Tsien RW (1985) Inactivation of calcium channels in mammalian heart cells: Joint dependence on membrane potential and intracellular calcium. J Physiol 364:395–411

Matsuda H, Noma A (1984) Isolation of calcium current and its sensitivity to monovalent cations in dialysed ventricular cells of guinea-pig. J Physiol 357:553–573

Matsuda H, Noma A, Kurachi Y, Irisawa H (1982) Transient depolarization and spontaneous voltage fluctuations in isolated single cells from guinea pig ventricles. Calcium-mediated membrane potential fluctuations. Circ Res 51:142–151

McLaughlin SGA, Szabo G, Eisenman G (1971) Divalent ions and the surface potential of charged phospholipid membranes. J Gen Physiol 58:667–687

Mentrard D, Vassort G, Fischmeister R (1984) Calcium-mediated inactivation of the calcium conductance in cesium-loaded frog heart cells. J Gen Physiol 83:105–131

Mironneau J, Eugene D, Mironneau C (1982) Sodium action potentials induced by calcium chelation in rat uterine smooth muscle. Pflügers Arch 395:232–238

Ohmori H (1984) Studies of ionic currents in the isolated vestibular hair cell of the chick. J Physiol 350:561–581

Prosser CL, Kreulen DL, Weigel RJ, Yau W (1977) Prolonged potentials in gastrointestinal muscles induced by calcium chelation. Am J Physiol 233:C19–24

Reuter H, Scholz H (1977) A study of the ion selectivity and the kinetic properties of the calcium dependent slow inward current in mammalian cardiac muscle. J Physiol 264:17–47

Rougier O, Vassort G, Garnier D, Gargouil YM, Coraboeuf E (1969) Existence and role of a slow inward current during the frog atrial action potential. Pflügers Arch 308:91–110

Sakmann B, Trube G (1984) Voltage-dependent inactivation of inward-rectifying single-channel currents in the guinea-pig heart cell membrane. J Physiol 347:659–683

Sigworth FJ (1980) The variance of sodium current fluctuations at the node of Ranvier. J Physiol 307:97–129

Yellen G (1984) Ionic permeation and blockade in Ca^{2+}-activated K^+ channels of bovine chromaffin cells. J Gen Physiol 84:157–186

Received October 19, 1985/Accepted May 7, 1986